Mechanism of metal-independent decomposition of organic hydroperoxides and formation of alkoxyl radicals by halogenated quinones

Ben-Zhan Zhu*†‡, Hong-Tao Zhao§, Balaraman Kalyanaraman§, Jun Liu*, Guo-Qiang Shan*, Yu-Guo Du*, and Balz Frei†

*State Key Laboratory of Environmental Chemistry and Ecotoxicology, Research Center for Eco-Environmental Sciences, Chinese Academy of Sciences, Beijing 100085, People's Republic of China; †Linus Pauling Institute, Oregon State University, Corvallis, OR 97331; and §Biophysics Research Institute, Medical College of Wisconsin, Milwaukee, WI 53226

Edited by Jack Halpern, University of Chicago, Chicago, IL, and approved December 18, 2006 (received for review July 2, 2006)

The metal-independent decomposition of organic hydroperoxides and the formation of organic alkoxyl radicals in the absence or presence of halogenated quinones were studied with electron spin resonance (ESR) and the spin-trapping agent 5,5-dimethyl-1-pyrroline *N*-oxide (DMPO). We found that 2,5-dichloro-1,4-benzoquinone (DCBQ) markedly enhanced the decomposition of *tert*-butylhydroperoxide (*t*-BuOOH), leading to the formation of the DMPO adducts with *t*-butoxyl radicals (*t*-BuO•) and methyl radicals (•CH_3). The formation of DMPO/*t*-BuO• and DMPO/•CH_3 was dose-dependent with respect to both DCBQ and *t*-BuOOH and was not affected by iron- or copper-specific metal chelators. Comparison of the data obtained with DCBQ and *t*-BuOOH with those obtained in a parallel study with ferrous iron and *t*-BuOOH strongly suggested that *t*-BuO• was produced by DCBQ and *t*-BuOOH through a metal-independent mechanism. Other halogenated quinones were also found to enhance the decomposition of *t*-BuOOH and other organic hydroperoxides such as cumene hydroperoxide, leading to the formation of the respective organic alkoxyl radicals in a metal-independent manner. Based on these data, we propose a mechanism for DCBQ-mediated *t*-BuOOH decomposition and formation of *t*-BuO•: a nucleophilic attack of *t*-BuOOH on DCBQ, forming a chloro-*t*-butylperoxyl-1,4-benzoquinone intermediate, which decomposes homolytically to produce *t*-BuO•. This represents a mechanism of organic alkoxyl radical formation not requiring the involvement of redox-active transition metal ions.

electron spin resonance spin-trapping | 2,5-dichloro-1,4-benzoquinone | 2,5-dichlorosemiquinone anion radical | reactive intermediate | metal chelators

Organic hydroperoxides (ROOH) can be formed both nonenzymatically by reaction of free radicals with polyunsaturated fatty acids and enzymatically by lipoxygenase- or cyclooxygenase-catalyzed oxidation of linoleic acid and arachidonic acid (1, 2). It has been shown that organic hydroperoxides can undergo transition metal ion-catalyzed decomposition to alkoxyl radicals (Reaction 1), which may initiate *de novo* lipid peroxidation or further decompose to α,β-unsaturated aldehydes that can react with and damage DNA and other biological macromolecules (1, 2).

$$\mathrm{ROOH} + \mathrm{Me}^{(n-1)+} \rightarrow \mathrm{RO}^{\bullet} + \mathrm{OH}^{-} + \mathrm{Me}^{n+}, \qquad [1]$$

where Me represents a transition metal, such as iron or copper.

Using the salicylate hydroxylation assay and electron spin resonance (ESR) spin-trapping methods, we reported previously that HO• can be produced from H_2O_2 by halogenated quinones independent of transition metal ions (3, 4). However, it is not clear whether halogenated quinones react in a similar fashion with organic hydroperoxides to produce alkoxyl radicals independent of transition metal ions.

Therefore, in the present study we addressed the following questions. (*i*) Can halogenated quinones enhance the decomposition of organic hydroperoxides to produce alkoxyl radicals? (*ii*) if so, is the production of alkoxyl radicals dependent or independent of transition metal ions? (*iii*) And what is the underlying molecular mechanism? To compare the similarities and differences to metal-dependent decomposition of ROOH, a parallel study with Fe(II)/ROOH was conducted.

Results and Discussion

ESR Spin-Trapping Evidence for the Formation of *t*-BuO• and •CH_3 from 2,5-Dichloro-1,4-benzoquinone (DCBQ) and *t*-BuOOH. Incubation of DCBQ (a model halogenated quinone; 0.1 mM) and *t*-BuOOH (a model short-chain organic hydroperoxide; 15 mM) with the spin-trapping agent DMPO (100 mM) led to the formation of two major radical adducts (Fig. 1). A similar ESR spectrum as shown in Fig. 1 was obtained when *t*-BuOOH was replaced by cumene hydroperoxide (data not shown). The spectra of the two major radical adducts and one minor radical adduct produced by DCBQ and *t*-BuOOH were identical to those produced by ferrous iron and *t*-BuOOH (cf. Fig. 6), which assigned the two major radical adducts in previous studies as the DMPO adducts with *t*-butoxyl radicals (*t*-BuO•) (DMPO/*t*-BuO•, $a^{\mathrm{H}} = 16.1$ G, $a^{\mathrm{N}} = 14.9$ G) and methyl radicals (•CH_3) (DMPO/•CH_3, $a^{\mathrm{H}} = 23.4$ G, $a^{\mathrm{N}} = 16.3$ G), and the minor radical adduct as the DMPO adduct with methoxy radicals (•OCH_3) (DMPO/•OCH_3, $a^{\mathrm{H}}_{\beta} = 10.7$ G, $a^{\mathrm{H}}_{\gamma} = 1.32$ G, and $a^{\mathrm{N}} = 14.5$ G) (5, 6). It should be noted that another minor radical adduct was also observed in both DCBQ and 2,6-dichloro-1,4-benzoquinone (2,6-DCBQ) systems but could not be detected in iron and other halogenated quinone systems (cf. Figs. 6 and 7). Further studies are needed to identify this radical adduct. In contrast, incubation of either compound alone (DCBQ or *t*-BuOOH) did not result in *t*-BuO• or •CH_3 formation (Fig. 1). The central signal in the spectrum shown in Fig. 1 for DCBQ alone was identified as the 2,5-dichlorosemiquinone anion radical (DCSQ•−) ($a^{\mathrm{H}} = 2.01$ G, $g = 2.0050$) (7). This DCSQ•− signal was also observed in the absence of DMPO. Addition of *t*-BuOOH to DCBQ led to a dramatic reduction of DCSQ•−, with the concomitant formation of *t*-BuO• and •CH_3 (Fig. 1). The formation of DMPO/*t*-BuO• and DMPO/•CH_3 was found to depend on the concentrations of both DCBQ and *t*-BuOOH (Figs. 2 and 3). Furthermore, formation

Author contributions: B.-Z.Z. designed research; B.-Z.Z., H.-T.Z., J.L., and G.-Q.S. performed research; B.K. Y.-G.D., and B.F. contributed new reagents/analytic tools; B.-Z.Z. analyzed data; and B.-Z.Z. wrote the paper.

The authors declare no conflict of interest.

This article is a PNAS direct submission.

Abbreviations: BCS, bathocuproine disulfonic acid; BPS, bathophenanthroline disulfonic acid; DCBQ, 2,5-dichloro-1,4-benzoquinone; DCHQ, 2,5-dichlorohydroquinone; DCSQ•−, 2,5-dichlorosemiquinone anion radical; DMF, dimethylformamide; DMPO, 5,5-dimethyl-1-pyrroline *N*-oxide; MPO, myeloperoxidase.

‡To whom correspondence may be addressed at: State Key Laboratory of Environmental Chemistry and Ecotoxicology, Research Center for Eco-Environmental Sciences, Chinese Academy of Sciences, P.O. Box 2871, Beijing 100085, People's Republic of China. E-mail: bzhu@rcees.ac.cn or benzhan.zhu@oregonstate.edu.

www.pnas.org/cgi/doi/10.1073/pnas.0605527104

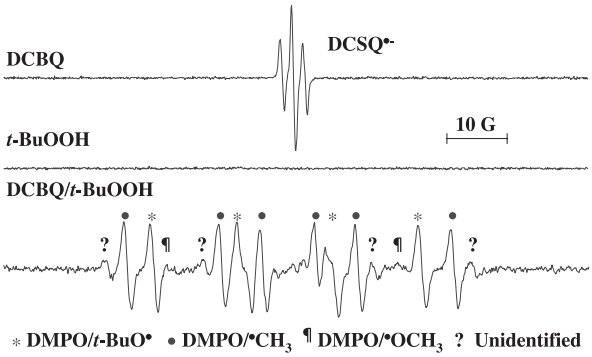

Fig. 1. ESR spectra of DMPO/*t*-BuO• and DMPO/•CH_3 produced by incubation of DMPO with DCBQ and *t*-BuOOH. Reactions were carried out at room temperature in Chelex-treated phosphate buffer (100 mM, pH 7.4). All reaction mixtures contained 100 mM DMPO. DCBQ, 0.1 mM; *t*-BuOOH, 15 mM. ESR spectra were recorded 1 min after the interactions between *t*-BuOOH and DCBQ at room temperature under normal room-lighting conditions. The central signal in the spectrum for DCBQ alone was identified as the 2,5-dichlorosemiquinone anion radical (DCSQ•$^-$) (a^H = 2.01 G; g = 2.0050). Hyperfine splitting constants for DMPO/*t*-BuO•, a^H = 16.1 G and a^N = 14.9 G; for DMPO/•CH_3, a^H = 23.4 G and a^N = 16.3 G; and for DMPO/•OCH_3, a^H_β = 10.7 G, a^H_γ = 1.32 G, and a^N = 14.5 G.

of DMPO/*t*-BuO• increased, whereas formation of DMPO/•CH_3 decreased, with increasing concentrations of DMPO (Fig. 4). Taken together, these results demonstrate that DCBQ can enhance the decomposition of *t*-BuOOH, leading to the formation of *t*-BuO• and •CH_3.

Formation of *t*-BuO• and •CH_3 from DCBQ and *t*-BuOOH Is Metal-Independent. Redox-active transition metals have been shown to be involved in the formation of *t*-BuO• and •CH_3 from *t*-BuOOH (1, 2, 5, 6). Therefore, the potential role of fortuitous transition metal ions in the DMPO/DCBQ/*t*-BuOOH reaction system was examined by the use of several structurally different and relatively specific metal chelators for iron and copper (1, 8–10). Neither the DMPO/*t*-BuO• signal nor the DMPO/•CH_3 signal produced by the DMPO/DCBQ/*t*-BuOOH system was reduced by the addition of various ferrous iron-specific chelators, namely, bathophenanthroline disulfonate (BPS), ferrozine, and ferene, or the cuprous copper-specific chelator bathocuproine disulfonate (BCS) (Fig. 5). In contrast, the formation of both DMPO/*t*-BuO• and DMPO/•CH_3 (Fig. 6) by the DMPO/Fe(II)/*t*-BuOOH system was almost completely inhibited by BPS, ferrozine, and ferene (Fig. 6). These results strongly suggest that contaminating transition metal ions are not responsible for *t*-BuO• and •CH_3 formation in incubations containing DCBQ and *t*-BuOOH.

Fig. 2. The formation of DMPO/*t*-BuO• and DMPO/•CH_3 depends on DCBQ concentration. Reactions were carried out at room temperature in Chelex-treated phosphate buffer (100 mM, pH 7.4). All reaction mixtures contained 100 mM DMPO and 15 mM *t*-BuOOH. DCBQ, 0.02, 0.1, and 0.5 mM. All of the other experimental conditions are the same as in Fig. 1.

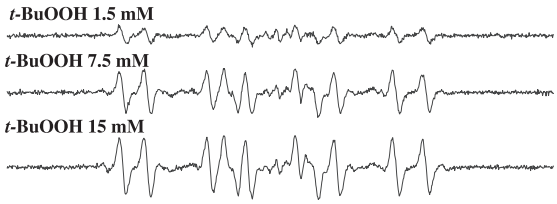

Fig. 3. The formation of DMPO/*t*-BuO• and DMPO/•CH_3 depends on *t*-BuOOH concentration. Reactions were carried out at room temperature in Chelex-treated phosphate buffer (100 mM, pH 7.4). All reaction mixtures contained 100 mM DMPO and 0.1 mM DCBQ. *t*-BuOOH, 1.5, 7.5, and 15 mM. All of the other experimental conditions are the same as in Fig. 1.

Metal-Independent Formation of *t*-BuO• and •CH_3 from Other Halogenated Quinones and *t*-BuOOH. The metal-independent production of *t*-BuO• and •CH_3 was not limited to DCBQ and *t*-BuOOH but was also observed with other halogenated quinones, i.e., tetrachloro-, trichloro-, 2,6-dichloro-, 2,3-dichloro-, 2-chloro-, tetrafluoro-, and tetrabromo-1,4-benzoquinone (Fig. 7). It is interesting to note that 2,5-dichloro- and 2,6-dichloro-1,4-benzoquinone were more efficient than 2,3-dichloro-1,4-benzoquinone in producing *t*-BuO• and •CH_3 (Fig. 7). In contrast, no *t*-BuO• and •CH_3 production was detected from *t*-BuOOH and the nonhalogenated quinone, 1,4-benzoquinone, or the methyl-substituted quinones 2,6-dimethyl- and tetramethyl-1,4-benzoquinone (data not shown).

Our observation that not only DCBQ but also other chlorinated quinones can react with organic hydroperoxides to produce alkoxyl radicals in a metal-independent manner has interesting biological implications. For example, many widely used chlorinated aromatic compounds such as hexachlorobenzene, polychlorinated phenols, including the widely used wood preservative pentachlorophenol (PCP), 2,4,5-trichlorophenoxyacetic acid (2,4,5-T), and 2,4-dichlorophenoxyacetic acid (2,4-D), can be metabolized *in vivo* to tetra-, di-, or mono-chlorinated quinones (7, 11, 12). Our data suggest that the chlorinated quinones may react with lipid hydroperoxides and exert toxic effects through enhanced production of alkoxyl radicals and hence increased lipid peroxidation. Additional work is needed to investigate whether these reactions occur and are relevant under physiological conditions or *in vivo*.

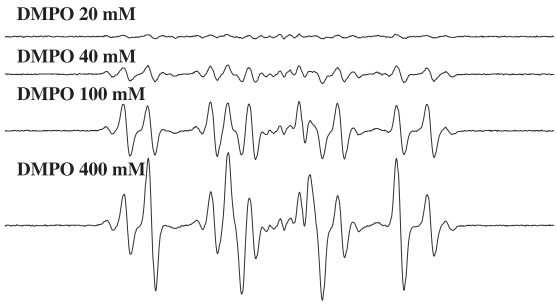

Fig. 4. The formation of DMPO/*t*-BuO• and DMPO/•CH_3 depends on DMPO concentration. Reactions were carried out at room temperature in Chelex-treated phosphate buffer (100 mM, pH 7.4). All reaction mixtures contained 0.1 mM DCBQ and 15 mM *t*-BuOOH. DMPO, 20, 40, 100, and 400 mM. All of the other experimental conditions are the same as in Fig. 1.

Fig. 5. Effect of iron- and copper-chelating agents on the ESR spectra of DMPO/*t*-BuO$^\bullet$ and DMPO/$^\bullet$CH$_3$ produced by incubation of DMPO with DCBQ and *t*-BuOOH. Reactions were carried out at room temperature in Chelex-treated phosphate buffer (100 mM, pH 7.4). All reaction mixtures contained 100 mM DMPO, 0.1 mM DCBQ, and 15 mM *t*-BuOOH. The metal-chelating agents (1 mM) were added to the reaction mixtures 2 min before *t*-BuOOH. All of the other experimental conditions are the same as in Fig. 1.

Molecular Mechanism of Metal-Independent Formation of *t*-BuO$^\bullet$ and $^\bullet$CH$_3$ from DCBQ and *t*-BuOOH. It is interesting to note that "spontaneous" formation of DCSQ$^{\bullet -}$ was observed once DCBQ was added to Chelex-treated phosphate buffer. The main source of the electron to reduce DCBQ may be water, via hydrolysis of DCBQ (13). Similar to the case of 1,4-benzoquinone, the "spontaneous" formation of DCSQ$^{\bullet -}$ may be due to H_2O addition to DCBQ to generate a hydroquinone, followed by redox interactions with DCBQ to yield DCSQ$^{\bullet -}$ (13, 14). Interestingly, the DCSQ$^{\bullet -}$ signal was markedly decreased by the addition of *t*-BuOOH, which was accompanied by formation of *t*-BuO$^\bullet$ (cf. Fig. 1). These data suggest that DCSQ$^{\bullet -}$ may directly react with *t*-BuOOH, reducing it to *t*-BuO$^\bullet$ (Reaction **2**), which is analogous to the Fe^{2+}-catalyzed decomposition of *t*-BuOOH to *t*-BuO$^\bullet$ (Reaction **3**):

$$t\text{-BuOOH} + \text{DCSQ}^{\bullet -} \rightarrow t\text{-BuO}^\bullet + \text{OH}^- + \text{DCBQ} \qquad [2]$$

$$t\text{-BuOOH} + \text{Fe}^{2+} \rightarrow t\text{-BuO}^\bullet + \text{OH}^- + \text{Fe}^{3+}\ . \qquad [3]$$

According to this mechanism, the production of *t*-BuO$^\bullet$ from *t*-BuOOH and DCBQ should depend on the concentration of DCSQ$^{\bullet -}$; i.e., the higher the concentration, the more *t*-BuO$^\bullet$ should be produced. Furthermore, the main product of this reaction should be DCBQ. However, no DMPO/*t*-BuO$^\bullet$ formation was detected from 2,5-dichlorohydroquinone (DCHQ, the reduced form of DCBQ) and *t*-BuOOH, although high concentrations of DCSQ$^{\bullet -}$ were produced during the autooxidation of

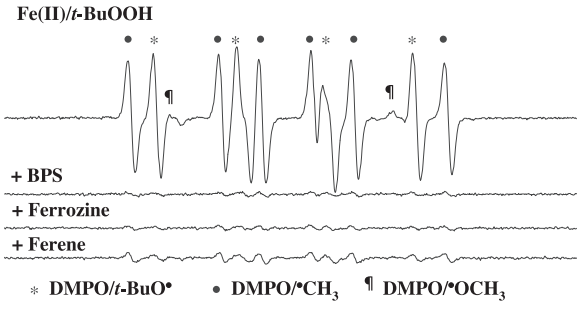

Fig. 6. Effect of iron-chelating agents on the ESR spectra of DMPO/*t*-BuO$^\bullet$ and DMPO/$^\bullet$CH$_3$ produced by incubation of DMPO with Fe(II) and *t*-BuOOH. Reactions were carried out at room temperature in Chelex-treated phosphate buffer (100 mM, pH 7.4). All reaction mixtures contained 100 mM DMPO, 0.1 mM Fe(II), and 15 mM *t*-BuOOH. The iron-chelating agents (1 mM) were added to the reaction mixtures 2 min before *t*-BuOOH. All of the other experimental conditions are the same as in Fig. 1.

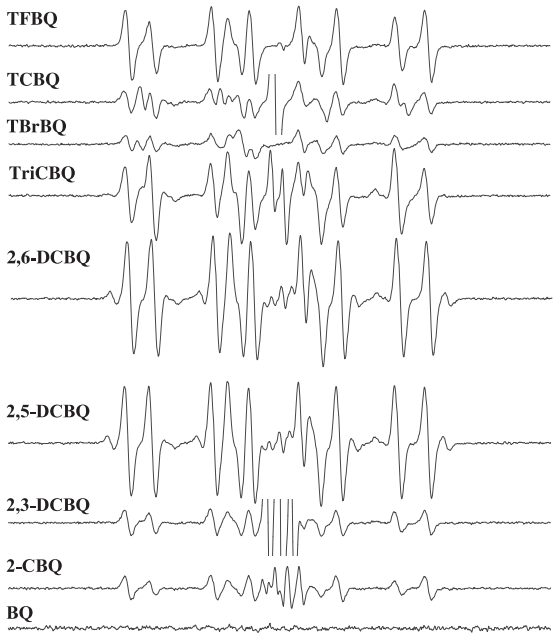

Fig. 7. ESR spectra of DMPO/*t*-BuO$^\bullet$ and DMPO/$^\bullet$CH$_3$ produced by incubation of DMPO with halogenated quinones and *t*-BuOOH. Reactions were carried out at room temperature in Chelex-treated phosphate buffer (100 mM, pH 7.4). All reaction mixtures contained 100 mM DMPO, 0.1 mM halogenated quinones, and 15 mM *t*-BuOOH. All of the other experimental conditions are the same as in Fig. 1. The central signals in each spectrum may represent the corresponding semiquinone anion radicals for each halogenated quinone compound. TCBQ, tetrachloro-1,4-benzoquinone; TriCBQ, trichloro-1,4-benzoquinone; 2,5-DCBQ, 2,5-dichloro-1,4-benzoquinone; 2,6-DCBQ, 2,6-dichloro-1,4-benzoquinone; 2,3-DCBQ, 2,3-dichloro-1,4-benzoquinone; 2-CBQ, 2-chloro-1,4-benzoquinone; TBrBQ, tetrabromo-1,4-benzoquinone; TFBQ, tetrafluoro-1,4-benzoquinone.

DCHQ (Fig. 8). Interestingly, if DCHQ was quickly oxidized to DCBQ with myeloperoxidase, DMPO/*t*-BuO$^\bullet$ could be detected (Fig. 8). Furthermore, the formation of DMPO/*t*-BuO$^\bullet$ was found to directly depend on DCBQ concentration (Fig. 2). These results suggest that DCBQ, but not DCSQ$^{\bullet -}$, may be essential for *t*-BuO$^\bullet$ production.

In addition, UV-visible spectral studies showed that there was a direct interaction between DCBQ and *t*-BuOOH, with the

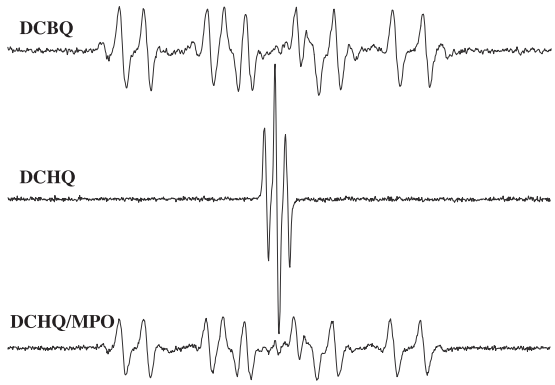

Fig. 8. DCSQ$^{\bullet -}$ may not be essential for the formation of DMPO/*t*-BuO$^\bullet$ and DMPO/$^\bullet$CH$_3$ adducts. Reactions were carried out in Chelex-treated phosphate buffer (100 mM, pH 7.4). All reaction mixtures contained 100 mM DMPO and 15 mM *t*-BuOOH. 2,5-dichlorohydroquinone (DCHQ, the reduced form of DCBQ), 0.1 mM; DCBQ, 0.1 mM; myeloperoxidase (MPO), 5 μg/ml. All of the other experimental conditions are the same as in Fig. 1.

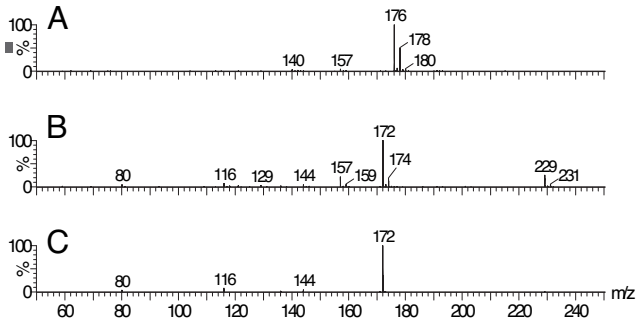

Fig. 9. The ESI-Q-TOF-MS spectra of DCBQ (*A*) and DCBQ with *t*-BuOOH (*B*) in CH_3COONH_4 buffer (pH 7.4, 0.1 M). DCBQ, 1 mM; *t*-BuOOH, 100 mM. Tandem mass spectrometric analysis showed that the peak at *m/z* 229 is unstable and can be readily fragmented to form the peak at *m/z* 172 (*C*) (collision energy, 17 eV).

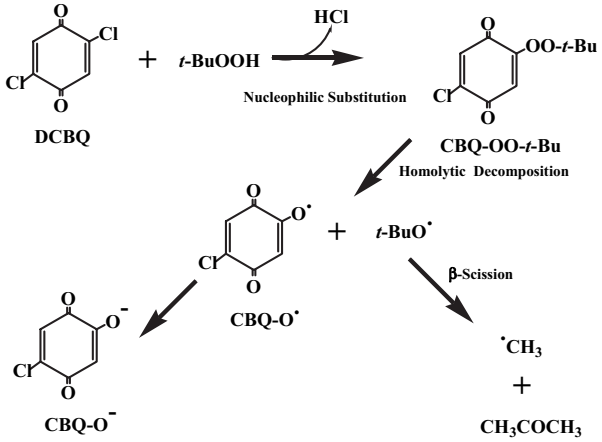

Scheme 1. Proposed mechanism for DCBQ-mediated *t*-BuOOH decomposition and formation of *t*-BuO• and •CH_3: A nucleophilic reaction may take place between DCBQ and *t*-BuOOH, forming a chloro-*t*-butylperoxyl-1,4-benzoquinone (CBQ-OO-*t*-Bu) intermediate, which can decompose homolytically to produce *t*-BuO• and 2-chloro-5-hydroxy-1,4-benzoquinone radical (CBQ-O•). CBQ-O• then disproportionate to form the ionic form of 2-chloro-5-hydroxy-1,4-benzoquinone ($CBQ\text{-}O^-$), and •CH_3 can be produced through β-scission of *t*-BuO•.

reaction mixture changing quickly from the original yellow color (λ_{max} = 272 nm) to a characteristic purple color (λ_{max} = 278 and 515 nm) in phosphate buffer (pH 7.4). The reaction intermediate and final products between DCBQ and *t*-BuOOH were identified by electrospray ionization quadrupole time-of-flight mass spectrometry (ESI-Q-TOF-MS). The mass spectrum of DCBQ in CH_3COONH_4 buffer (pH 7.4, 0.1 M) is characterized by a two-chlorine isotope cluster at *m/z* 176 and a small one-chlorine isotope cluster at *m/z* 157 (Fig. 9*A*). The addition of *t*-BuOOH to DCBQ led to a complete disappearance of the molecular ion peak cluster at *m/z* 176, a significant increase (11-fold) in the intensity of peak cluster at *m/z* 157, and the appearance of two new one-chlorine isotope clusters at *m/z* 229 and 172 (Fig. 9*B*). Tandem mass spectrometric analysis showed that the peak at *m/z* 229 is unstable and can be readily fragmented to form the peak at *m/z* 172 (Fig. 9*C*), whereas the peak at *m/z* 157 is fragmented to form the peak at *m/z* 121, which corresponds to the loss of HCl. Similar ESI-MS results were observed when DCBQ was substituted with 2,6-DCBQ (data not shown). These results indicate that the major reaction intermediate between DCBQ and *t*-BuOOH was probably chloro-*t*-butylperoxyl-1,4-benzoquinone (CBQ-OO-*t*-Bu) (peak clusters at *m/z* 229), and the major reaction product between DCBQ and *t*-BuOOH was probably the ionic form of 2-chloro-5-hydroxy-1,4-benzoquinone (CBQ-OH) (peak clusters at *m/z* 157). This was confirmed by comparing with the authentic CBQ-OH synthesized according to the method in refs. 15 and 16, which showed the same ESI-MS profile and the same retention time in HPLC (see *Material and Methods*). However, we could not identify a compound corresponding to *m/z* 172 from the reaction mixture between DCBQ and *t*-BuOOH. This may indicate that the fragment ion at *m/z* 172 is solely derived from the peak at *m/z* 229 during ESI-MS analysis process, and it was probably the methyl adduct of the decomposition intermediate 2-chloro-5-hydroxy-1,4-benzoquinone radical (CBQ-O•) (see below).

Thus, the metal-independent production of *t*-BuO• by DCBQ and *t*-BuOOH appears not to occur through a semiquinone-mediated reaction. Based on the above experimental results, a mechanism is proposed for DCBQ-mediated *t*-BuOOH decomposition and formation of *t*-BuO• and •CH_3: A nucleophilic reaction may take place between DCBQ and *t*-BuOOH, forming a chloro-*t*-butylperoxyl-1,4-benzoquinone (CBQ-OO-*t*-Bu) intermediate, which can decompose homolytically to produce *t*-BuO• and 2-chloro-5-hydroxy-1,4-benzoquinone radical (CBQ-O•). CBQ-O• then disproportionate to form the ionic form of 2-chloro-5-hydroxy-1,4-benzoquinone ($CBQ\text{-}O^-$), and •CH_3 can be produced through β-scission of *t*-BuO• (Scheme 1). It should be noted that CBQ-O• could not be detected under our current experimental conditions. The reason may be that either its half-life span is too short or its steady-state concentration is too low. Further studies are needed to identify this radical intermediate.

Materials and Methods

Chemicals. 2,5-dichloro-1,4-benzoquinone (DCBQ, or 2,5-dichloro-*p*-benzoquinone), 2,6-dichloro-1,4-benzoquinone (2,6-DCBQ), 2,3-dichloro-1,4-benzoquinone (2,3-DCBQ), 2-chloro-1,4-benzoquinone (CBQ), 1,4-benzoquinone (BQ), trichloro-1,4-benzoquinone (TriCBQ), tetrachloro-1,4-benzoquinone (TCBQ), tetrabromo-1,4-benzoquinone (TBrBQ), tetrafluoro-1,4-benzoquinone (TFBQ), 2,6-dimethyl-1,4-benzoquinone, tetramethyl-1,4-benzoquinone, 5,5-dimethyl-1-pyrroline *N*-oxide (DMPO), and bathocuproine disulfonate (BCS) were purchased from Aldrich. *tert*-Butylhydroperoxide (*t*-BuOOH), cumene hydroperoxide (CuOOH), dimethylformamide (DMF), ferrozine, ferene, and bathophenanthroline disulfonate (BPS) were purchased from Sigma. The chemicals were used as received without further purification.

Synthesis of 5-Chloro-2-hydroxy-1,4-benzoquinone (CBQ-OH). CBQ-OH was synthesized as described (15, 16). 1,2,4-Trihydroxy-benzene (1g) was refluxed with *N*-chlorosuccinimide (1.06 g) and dibenzoylperoxide (10 mg) in ether (100 ml) for 3 h. The reaction mixture was cooled and filtered to remove most of the succinimide. The organic phase was washed with water, dried over anhydrous sodium sulfate, and evaporated under reduced pressure to yield crude 5-chloro-2-hydroxy-hydroquinone, which was purified by silica gel column chromatography using ethyl acetate as an eluent. This product was purified further by crystallization from ether-hexane. CBQ-OH was prepared by allowing 5-chloro-2-hydroxy-hydroquinone to spontaneously oxidize in air (16). CBQ-OH was characterized by ^{1}HNMR (400 MHz, $CDCl_3$), 6.85 (s, 1H, Ar-H), 6.60 (s, 1H, Ar-H); ESI-MS, one-chlorine isotope cluster at *m/z* 157; and MS/MS, major fragment ion at *m/z* 121.

ESR Studies. The basic system used in this study consisted of halogenated quinones dissolved in DMF (final DMF concentration in the reaction mixture, 1%), *t*-BuOOH, and the spin-

trapping agent DMPO (100 mM), with or without metal-chelating agents, in Chelex-treated phosphate buffer (100 mM, pH 7.4) at room temperature. The metal-chelating agents were added to the reaction mixture 2 min before *t*-BuOOH, and the solutions were air-saturated. ESR spectra were recorded 1 min after the interactions between *t*-BuOOH and DCBQ (or other halogenated quinones) at room temperature under normal room-lighting conditions on a Bruker ER 200 D-SRC spectrometer operating at 9.8 GHz and a cavity equipped with a Bruker Aquax liquid sample cell. Typical spectrometer parameters were as follows: scan range, 100 G; field set, 3,470 G; time constant, 200 ms; scan time, 100 s; modulation amplitude, 1.0 G; modulation frequency, 100 kHz; receiver gain, 1.25×10^4; and microwave power, 9.8 mW.

UV-Visible Spectral Analysis. The interaction between halogenated quinones and *t*-BuOOH was monitored in a UV-visible spectrophotometer (Beckman DU-640), using Chelex-treated phosphate buffer (100 mM, pH 7.4) at room temperature.

ESI-Q-TOF MS. Analysis by electrospray ionization quadrupole time-of-flight mass spectrometry of the reaction intermediate and final products between DCBQ and *t*-BuOOH was performed on a Micromass Q-TOF mass spectrometer. MS and MS/MS spectra were acquired in negative-ion mode. The reactions between DCBQ (1 mM) and *t*-BuOOH (100 mM) were conducted in CH_3COONH_4 buffer (pH 7.4, 0.1 M) at room temperature, and the sample solutions were directly introduced 1 min after the reaction at 30 μl/min using a Z-spray ESI source. Capillary and sample cone voltages were 2.5 kV and 30 V; source and desolvation temperatures were 80°C and 200°C. Nitrogen was used as the drying gas. The collision gas was argon at the pressure of 5.0×10^{-5} Torr, and the collision energy was 10 V. Both the high and low resolution for mass filter were set at 5.0 V. The pressure in the TOF cell was lower than 3.0×10^{-7} Torr (1 Torr = 133.322 Pa). Full-scan spectra were recorded in profile mode. The range between *m*/*z* 50 and 450 was recorded at a resolution of 5,000 (FWHM), and the accumulation time was 1 s per spectrum. For MS/MS studies, the quadrupole was used to select the parent ions, which were subsequently fragmented in a hexapole collision cell by using argon as the collision gas and an appropriate collision energy (typically 10–20 eV). Data acquisition and analysis were carried out by using MassLynx software (Waters; Version 4.0).

HPLC Conditions. Samples were analyzed with an HPLC apparatus equipped with a model 2996 photodiode array detector (Waters 2695 XE). Samples were directly transferred into minivials and immediately injected onto a SUPELCOSIL LC-18 C_{18} column (Sigma; 4.6×250 mm; pore size of 60 μm) equilibrated with 50 mM acetic acid. Samples were eluted at a flow rate of 1 ml/min with a 50 mM acetic acid-acetonitrile gradient [acetonitrile concentrations of 0% (isocratic, 5 min), 0–70% (linear, 5 min), 70% (isocratic, 5 min), and 100% (isocratic, 5 min)]. The absorbance was monitored between 200 and 700 nm. Sample retention times and absorption maxima were compared with those of standard compounds. The HPLC standard 5-chloro-2-hydroxy-1,4-benzoquinone was distinguished by its retention time of 8.43 min and its absorption maxima of 275 nm.

We acknowledge the technical help provided by Drs. Christopher Felix, Joy Joseph, and Renliang Zhang, and Ms. Rui Guo. This work was supported by the Hundred-Talent Project; the Chinese Academy of Sciences; National Natural Science Foundation of China Grants 20647004 and 20621703; National Institutes of Health Grants ES11497, RR01008, and ES00210 (to B.-Z.Z.); National Natural Science Foundation of China Grant 20572128 (to Y.-G.D.); and National Center for Complementary and Alternative Medicine Center of Excellence Grant AT002034 (to B.F.).

1. Halliwell B, Gutteridge JMC (1999) *Free Radicals in Biology and Medicine* (Oxford Univ Press, Oxford).
2. Marnett LJ (2000) *Carcinogenesis* 21:361–370.
3. Zhu BZ, Kitrossky N, Chevion M (2000) *Biochem Biophys Res Commun* 270:942–946.
4. Zhu BZ, Zhao HT, Kalyanaraman B, Frei B (2002) *Free Radical Biol Med* 32:465–473.
5. Guo Q, Qian SY, Mason RP (2003) *J Am Soc Mass Spectrom* 14:862–871.
6. Chen YR, Mason RP (2002) *Biochem J* 365:461–469.
7. Juhl U, Blum JK, Butte W, Witte I (1991) *Free Radical Res Commun* 11:295–305.
8. Mohindru A, Fisher JM, Rabinowitz M (1983) *Nature* 303:64–65.
9. Graf E, Mahoney JR, Bryant RG, Eaton JW (1984) *J Biol Chem* 259:3620–3624.
10. Dean RT, Nicholson P (1994) *Free Radical Res* 20:83–101.
11. van Ommen B, Adang AE, Brader L, Posthumus MA, Muller F, van Bladeren PJ (1986) *Biochem Pharmacol* 35:3233–3238.
12. Haugland RA, Schlemm DJ, Lyons RP, III, Sferra PR, Chakrabarty AM (1990) *Appl Environ Microbiol* 56:1357–1362.
13. Sarr DH, Kazunga C, Charles MJ, Pavlovich JG, Aitken MD (1995) *Environ Sci Technol* 29:2735–2740.
14. Brunmark A, Cadenas E (1987) *Free Radical Biol Med* 3:169–180.
15. Joshi DK, Gold MH (1993) *Appl Environ Microbiol* 59:1779–1785.
16. Zaborina O, Daubaras DL, Zago A, Xun L, Saido K, Klem T, Nikolic D, Chakrabarty AM (1998) *J Bacteriol* 180:4667–4675.